

Formation of rogue waves from the locally perturbed condensate

A. A. Gelash^{1,2*}

¹*Novosibirsk State University, Novosibirsk, 630090, Russia and*

²*Institute of Thermophysics, SB RAS, Novosibirsk, 630090, Russia*

(Dated: December 14, 2024)

The one-dimensional focusing nonlinear Schrödinger equation (NLSE) on an unstable condensate background is among the most important models of rogue wave formation. The complete integrability of the NLSE via inverse scattering transform enables the decomposition of the initial conditions into elementary nonlinear modes: breathers and continuous spectrum waves. The small localized condensate perturbations (SLCP) that grow as a result of modulation instability (MI) have been of fundamental interest in nonlinear physics for many years. Here, we demonstrate that the so-called superregular NLSE breathers play the key role in the dynamics of a wide class of SLCP. During the nonlinear stage of MI development, collisions of superregular breathers lead to the formation of rogue waves. We present scenarios of rogue wave formation for randomly distributed superregular breathers as well as for artificially prepared initial conditions. For the latter case, we present an analytical description based on the exact expressions found for the space-phase shifts that breathers acquire after collisions with each other. Finally, the presence of superregular breathers in arbitrary-type condensate perturbations is demonstrated by solving the Zakharov-Shabat eigenvalue problem with high numerical accuracy.

PACS numbers: 05.45.Yv, 02.30.Ik, 42.81.Dp, 47.35.Fg

Introduction

The formation of extreme-amplitude waves is among the most remarkable phenomenon in the physics of wave processes. In the linear case, these events may appear only as a result of simple wave interference, whereas the interactions of nonlinear waves exhibit a wide range of nontrivial mechanisms, such as the development of modulation instability (MI) and nonlinear wave focusing [1, 2]. The so-called *rogue (freak)* waves are of special interest as they suddenly appear from relatively weak perturbations of a calm background. This unusual phenomenon has been observed experimentally in different nonlinear media, such as optical fiber with Kerr nonlinearity, Bose-Einstein condensate and the surface of a fluid [3–5].

The one-dimensional focusing nonlinear Schrödinger equation (NLSE):

$$i\psi_t - \frac{1}{2}\psi_{xx} - (|\psi|^2 - A^2)\psi = 0, \quad (1)$$

is one of the most fundamental mathematical models describing weakly nonlinear wave propagation accompanied by the formation of rogue waves. Here, $\psi(t, x)$ is the complex-valued wavefield envelope, t and x are the time and space coordinates, and the meaning of the constant A is discussed below.

In the early 1970's, V.E. Zakharov and A.B. Shabat found that the NLSE with infinite line vanishing boundary conditions (BC) can be completely integrated using a very powerful technique – the inverse scattering transform (IST) [6]. In 1977, E.A. Kuznetsov [7] and later Y.C. Ma, T. Kawata and H. Inoue [8, 9], studied the case of the NLSE on the so-called *condensate* background – a simple quasi-monochromatic plane wave. In this work,

we write the condensate solution of the equation (1) as $\psi_0(t, x) = A$, where A is the background amplitude (ψ describes the envelope of the physical wavefield), which we assume to be real without loss of generality. The limit of vanishing BC corresponds to the case $A = 0$. The condensate is unstable with respect to long-wave perturbations (MI) with the following growth rate:

$$\Gamma(k) = k\sqrt{A^2 - k^2/4}, \quad (2)$$

where k is the perturbation wave number. In the region $0 < k < 2$, the amplitude of these perturbations grows $\sim e^{\Gamma t}$ in the initial (linear) stage. The nonlinear stage of MI development may lead to the formation of rogue waves (see, for instance, [2]).

The NLSE on the condensate background has a large family of exact solutions, such as Peregrine [10], Kuznetsov-Ma [7, 8] and Akhmediev [11] breathers. Moreover, the IST links the initial NLSE wavefield with the so-called *scattering data*, which play the role of non-interacting nonlinear modes, similar to Fourier harmonics in linear wave theory. The evolution of scattering data is trivial and enables N -breather solutions to be found analytically and the general Cauchy problem to be solved implicitly via the integral Gelfand-Levitan-Marchenko equations (GLME). The scattering data are represented by the discrete (breathers) and continuous (nonlinear dispersive waves) parts of the eigenvalue spectrum of the Zakharov-Shabat auxiliary linear system (ZH system).

However, the nontrivial interactions of breathers and continuous spectrum waves with unstable condensate background and between each other makes the system evolution complicated and produces many fundamental questions. One question is the long-term evolution of un-

stable small localized condensate perturbations (SLCP). In the mentioned paper [7], E.A. Kuznetsov suggested that the MI in this case is driven by the unstable part of continuous spectrum waves and leads (in the final stage) to a sort of local (i.e., in the area of the initial perturbation) Fermi-Pasta-Ulam (FPU) recurrence of the unperturbed condensate. In 2017, E.A. Kuznetsov presented a qualitative explanation that such local recurrence can be explained by representation of the condensate background as a particular limiting case of a soliton lattice [12]. Additional important results were recently obtained by G. Biondini et al. [13, 14]. They analytically described the MI of continuous spectrum waves via asymptotic analysis of the GLME on the condensate background.

For a long time, the role of discrete spectrum solutions in the development of SLCP was attributed to only a particular class of Peregrine-type multi-breather rational solutions. They are known as the simplest analytical model of rogue wave formation and are also called *rational rogue waves* (see, for instance, [15, 16]). In 2010, V.I. Shrira and V.V. Geogjaev expanded this approach to the wide subclass of Kuznetsov-Ma breathers [17]. The pure rational rogue wave scenario of MI development leads to complete FPU recurrence, and the general scenario with Kuznetsov-Ma breathers demonstrates long-term standing oscillations.

Recently, V.E. Zakharov and A.A. Gelash found that NLSE breathers may be hidden in SLCP at the moment of their pairwise collisions. Based on this observation, they suggested a new scenario of MI development, which describes the formation of moving interacting breathers at the intermediate stage and long-term local recurrence to the unperturbed condensate [18, 19]. The experimental confirmation of these theoretical results was obtained simultaneously in optics and hydrodynamics by B. Kibler et al. [20]. The later study of generalized NLSE and modified KdV models revealed the universal character of superregular breathers [21, 22]. However, the role of superregular breathers in the development of arbitrary-type (random) SLCP remains unclear. In this paper, we prove that superregular breathers are contained in a wide class of arbitrary-type initial conditions and demonstrate that they play the key role in the formation of rogue waves from the locally perturbed condensate.

Breather solutions of the NLSE

The eigenvalue problem for a ZH system can be written in the following form:

$$\widehat{L}\Phi = \lambda\Phi, \quad \widehat{L} = \begin{pmatrix} 1 & 0 \\ 0 & -1 \end{pmatrix} \frac{\partial}{\partial x} - \begin{pmatrix} 0 & \psi \\ \psi^* & 0 \end{pmatrix}. \quad (3)$$

Here, $\Phi(x, t, \lambda)$ is the matrix wave function (eigenfunction), and λ is the spectral parameter defined on the

two-sheeted Riemann surface containing a branchcut on the interval $[-A, A]$. The general N -breather solution of the NLSE (1) ψ_N corresponds to N discrete eigenvalues λ_n on the right half of the λ -plane and can be written in the following form [18, 19]:

$$\psi_N = A + 2 \frac{\det \widetilde{M}_{1,2}}{\det M}, \quad \text{where } M_{nm} = \frac{(\mathbf{q}_n \cdot \mathbf{q}_m^*)}{\lambda_n + \lambda_m^*}, \quad (4)$$

$$\text{and } \widetilde{M}_{\alpha,\beta} = \begin{pmatrix} 0 & q_{1,\beta} & \cdots & q_{n,\beta} \\ q_{1,\alpha}^* & & & \\ \vdots & & M_{nm}^T & \\ q_{n,\alpha}^* & & & \end{pmatrix}.$$

Here, the two-component vectors $\mathbf{q}_n = (q_{n,1}, q_{n,2})$ are given by:

$$q_{n,1} = e^{-\phi_n} - \frac{iAe^{\phi_n}}{\lambda_n + \zeta_n}, \quad q_{n,2} = -\frac{iAe^{-\phi_n}}{\lambda_n + \zeta_n} + e^{\phi_n}, \quad (5)$$

$$\phi_n = \zeta_n x - \text{Re}[\zeta_n]x_{0,n} - i\lambda_n \zeta_n t - i\theta_n/2,$$

where the functions $\zeta_n = \sqrt{A^2 - \lambda_n^2}$ define the branchcut of the spectral parameter plane. Each n -th breather is characterized by four real parameters: $\text{Re}[\lambda_n]$, $\text{Im}[\lambda_n]$, $x_{0,n}$ and θ_n . The complex eigenvalue λ_n is responsible for the breather amplitude, velocity and period of oscillations, while $x_{0,n}$ and θ_n describe the breather position in space and its complex *internal* phase.

In the main text of the paper, we use the straightforward expression for the single-breather solution defined by one set of parameters, namely λ , x_0 , θ , and by one vector, $\mathbf{q} = (q_1, q_2)$:

$$\psi_1 = e^{-i\theta_c} \left(A - 2(\lambda + \lambda^*) \frac{q_1^* q_2}{|q_1|^2 + |q_2|^2} \right). \quad (6)$$

Here, θ_c is the additional phase parameter, which is the general phase of the condensate and usually is taken to be zero. However, in this work, θ_c is very useful in the description of breather interactions – see the text below. Furthermore, the internal breather phase θ cannot be written as common multiplier $e^{i\theta}$ for a single breather, as shown by (6) or Eq.(2) in the Appendix.

The Peregrine, Kuznetsov-Ma and Akhmediev breathers are particular cases of the general solution (6) at $\lambda = A$; $\text{Re}[\lambda] > A$, $\text{Im}[\lambda] = 0$; and $\text{Re}[\lambda] < A$, $\text{Im}[\lambda] = 0$, respectively. The dynamics of these breathers are well known – see, for instance, [19]. The Akhmediev breather describes periodic condensate perturbations, whereas the Peregrine and Kuznetsov-Ma breathers are standing oscillating objects localized in space. The minimal amplitude of the Kuznetsov-Ma breather is controlled by the distance from the eigenvalue λ to the branch point A , so the mentioned Kuznetsov-Ma breather scenario of SLCP development can be implemented only when the eigenvalues distributed on the real axes are close to the branch point.

As found in [18], for certain parameters, \tilde{N} pairs of breathers can describe the development of MI from SLCP. These special types of exact solutions are called \tilde{N} -pair superregular breathers. In the simplest case, the superregular scenario of MI development is described by one pair of breathers with symmetrically located (about the branchcut) eigenvalues and the following space-phase synchronization:

$$\begin{aligned} \lambda_1 &= \mu + \varepsilon i, & \lambda_2 &= \mu - \varepsilon i; & \mu &< A, & \varepsilon &\ll 1, & (7) \\ x_{0,1} &= x_{0,2} = 0, & \theta_1 &= \theta_2 = \pi. \end{aligned}$$

In Fig. 1, we present an example of a symmetric one-pair superregular solution (7) with $\mu = 1/\sqrt{2}$, which corresponds to the maximum of the MI growth rate (2) at $k_{max} = \sqrt{2}$ (see the detailed discussion of the superregular perturbation growth rate in the Appendix).

In the general case, a pair of superregular eigenvalues is located at the parametric curves defined by:

$$\text{Re}[\lambda] = \frac{A \cos \alpha}{2} \left(r + \frac{1}{r} \right), \quad \text{Im}[\lambda] = \pm \frac{A \sin \alpha}{2} \left(r - \frac{1}{r} \right). \quad (8)$$

Here, the auxiliary angle variable $\alpha \in (0, \pi/2)$ and \pm signs correspond to the first and second breather in the pair (see Appendix, where the derivation of expressions (8) is presented).

The continuous spectrum eigenvalues of the ZH system (3) are located at the imaginary axis plus the branchcut. The unstable continuous spectrum waves correspond only to the eigenvalues on the branchcut [7]. The imaginary axis eigenvalues are associated with stable continuous spectrum waves, which do not have a significant impact on the development of SLCP.

Breather interactions: space-phase shifts

To analyze multi-breather interactions, we need exact expressions describing the space-phase shifts that breathers acquire after collisions with each other. Such formulas have been known for soliton interactions on zero background since the paper of V.E. Zakharov and A.B. Shabat [6]. However, the derivation of the breather space-phase shifts was skipped in the work devoted to the IST of the NLSE on the condensate background [7–9]. To the best of our knowledge, these expressions have not been reported.

We solve the space-phase shifts problem using the standard technique: asymptotic analysis of the two-breather solution, which can be obtained from (4) at $N = 2$. Considering the asymptotic states of separate breathers at $t \rightarrow \pm\infty$, we find the following expressions that describe the space shift $\Delta x_{0,2}$ and phase shifts $\Delta\theta_2, \Delta\theta_{c,2}$ that

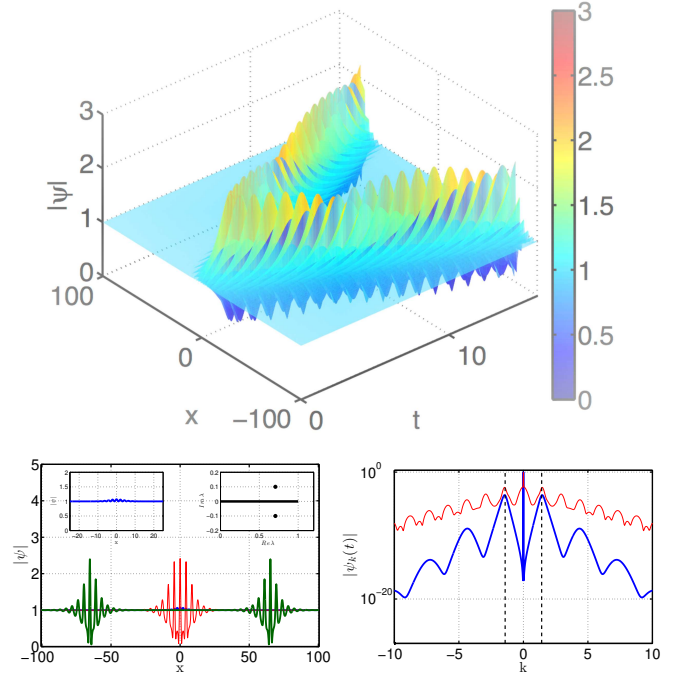


FIG. 1: Perturbation development driven by the simplest one-pair superregular breather solution. Top picture demonstrates the whole space-time evolution of the wavefield. The left picture shows the amplitude profile of the solution at the initial moment of time ($t = 0$, bold blue line), at an intermediate stage ($t = 2$, thin red line), and at the final stage ($t = 13$, bold green line) of MI development. The corresponding Fourier spectra for the initial and intermediate stages are shown in the right picture (black dotted line corresponds to the value of k_{max}). The magnification of the initial condensate perturbation at $t = 0$ and the eigenvalues of breathers are shown in the insets.

breather 2 acquires after collision with the breather 1:

$$\Delta x_{0,21} = \frac{1}{2\text{Re}[\zeta_2]} \ln \left(\frac{s_1 - s_3}{s_2 - s_4} \right), \quad (9)$$

$$\Delta\theta_{21} = 2\text{Arg}[i^2(p_1 - p_2)]; \quad \Delta\theta_{c,21} = -4\text{Arg}[i(\lambda_1 + \zeta_1)].$$

Here, the coefficients s_1, s_2, s_3, s_4, p_1 , and p_2 have the following cumbersome dependence on the eigenvalues λ_1 and λ_2 :

$$\begin{aligned} s_1 &= (A^4 + |\lambda_1 + \zeta_1|^2 \cdot |\lambda_2 + \zeta_2|^2) \cdot |\lambda_1 + \lambda_2^*|^2 + \\ &\quad + A^2 (|\lambda_1 + \zeta_1|^2 + |\lambda_2 + \zeta_2|^2) \cdot |\lambda_1 - \lambda_2|^2, \\ s_2 &= A^2 (|\lambda_1 + \zeta_1|^2 + |\lambda_2 + \zeta_2|^2) \cdot |\lambda_1 + \lambda_2^*|^2 + \\ &\quad + (A^4 + |\lambda_1 + \zeta_1|^2 \cdot |\lambda_2 + \zeta_2|^2) \cdot |\lambda_1 - \lambda_2|^2, \\ s_3 &= A^2 (\lambda_1 + \lambda_1^*) (\lambda_2 + \lambda_2^*) \cdot [(\lambda_1 + \zeta_1)(\lambda_2 + \zeta_2) + \\ &\quad + (\lambda_1^* + \zeta_1^*)(\lambda_2^* + \zeta_2^*)], \\ s_4 &= A^2 (\lambda_1 + \lambda_1^*) (\lambda_2 + \lambda_2^*) \cdot [(\lambda_1 + \zeta_1)(\lambda_2^* + \zeta_2^*) + \\ &\quad + (\lambda_1^* + \zeta_1^*)(\lambda_2 + \zeta_2)], \\ p_1 &= \{A^2 (\lambda_2 + \zeta_2 + \lambda_1^* + \zeta_1^*) + |\lambda_1 + \zeta_1|^2 (\lambda_2^* + \zeta_2^*) + \\ &\quad + |\lambda_2 + \zeta_2|^2 (\lambda_1 + \zeta_1)\} / \{|\lambda_1 + \lambda_2^*|^2\}, \\ p_2 &= \frac{(A^2 + |\lambda_1 + \zeta_1|^2) (\lambda_2 + \zeta_2 + \lambda_2^* + \zeta_2^*)}{(\lambda_1 + \lambda_1^*) (\lambda_2 + \lambda_2^*)}. \end{aligned}$$

We use additional general phase θ_c (defined in (6)) for the second breather to describe how the first breather reverses the condensate phase after itself. One can check that as $A \rightarrow 0$, expressions (9) become well-known soliton space-phase shifts, so the two phases θ_2 and $\theta_{c,2}$ form a single soliton phase.

Rogue wave formation as a result of superregular breather collisions

Collisions of NLSE breathers with particular phases can produce typical rogue waves [2, 23, 24]. The formation of SLCP by superregular solutions is the back side of this process. Indeed, depending on the sum of the breather phases, $\theta_1 + \theta_2$, the amplitude profile at the moment of collision can vary from a small perturbation to a rogue wave of extreme amplitude, which we discussed in [20] and illustrate in Fig. 2.

Nevertheless, the scenario where moving NLSE breathers appear from SLCP and then produce rogue waves by collision with each other has not been studied. We found that pairs of superregular breathers synchronized inside each pair can be additionally synchronized between each other to produce a rogue wave during the nonlinear stage of MI development. Such two-step synchronization accounts for the space-phase shifts (9), which we can perform analytically – see the details in the Appendix. This new scenario of rogue wave formation for the simplest four-breather model with symmetric eigenvalues is presented in Fig. 3. Perturbations generate four breathers as a result of MI; then, two of the breathers move towards each other and collide to produce the rogue wave.

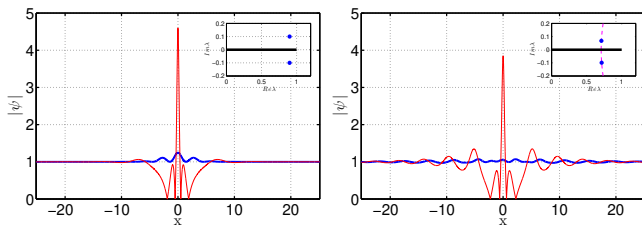


FIG. 2: Amplitude profiles of two-breather collision. Bold blue lines correspond to superregular synchronization ($\theta_1 + \theta_2 = \pi$), while thin red lines show the rogue wave formation at $\theta_1 + \theta_2 = 2\pi$. The inset pictures show the breather eigenvalues. The left and right pictures correspond to symmetric and nonsymmetric breathers. The dashed magenta line shows that the discrete eigenvalues in the nonsymmetric case lie on the parametric curves (8).

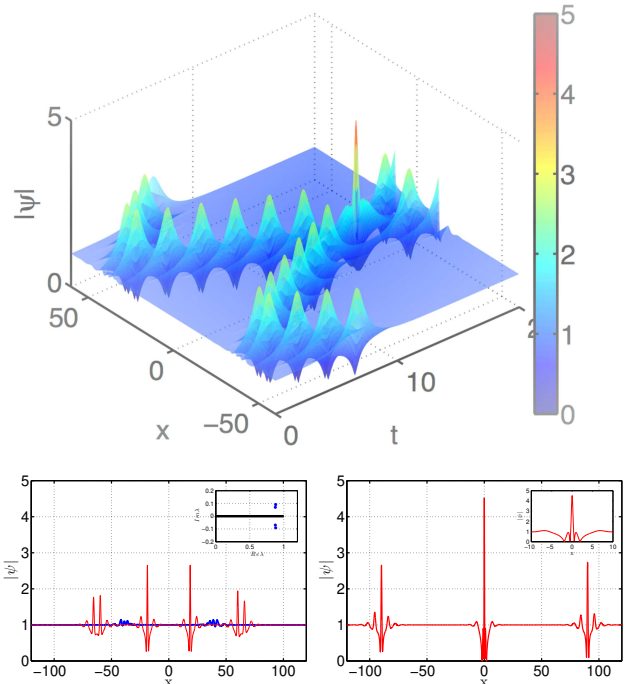


FIG. 3: New scenario of rogue wave formation from the locally perturbed condensate. Top picture demonstrates the whole space-time evolution of the wavefield. The left picture represents the initial condensate perturbations – two pairs of superregular breathers (solid blue line), the intermediate stage at $t = 7$ (thin red lines) and breather eigenvalues (inset picture). The right picture shows the moment of rogue wave formation at $t = 15$.

Rogue wave formation from the randomly perturbed condensate

The suggested scenario of rogue wave formation can be observed not only for manually synchronized breathers but also for the random distribution of superregular condensate perturbations. In Fig. 4, we present an example of 16-breather MI development. At the initial moment of time, the condensate is locally perturbed by 8 superregular pairs that are randomly distributed in space – see the left picture. In this case, the breather phases in each pair can be synchronized separately, so we can generate the initial conditions without using formulas (9). In the right picture, we show the most significant rogue wave observation over 100 random initial condition runs. Note that the simulation of the multi-breather solution by exact formulas is an ill-conditioned problem at a large number of breathers (we recently discussed the same problem for solitons in [25] and [26]). Here, we use the Zakharov-Shabat dressing method (an alternative formulation of the N -breather solution (4) – see our previous works [18, 19] for details) supplemented with 100-digits precession arithmetic to mitigate the numerical instability and to generate accurate 8-pair superregular initial

conditions.

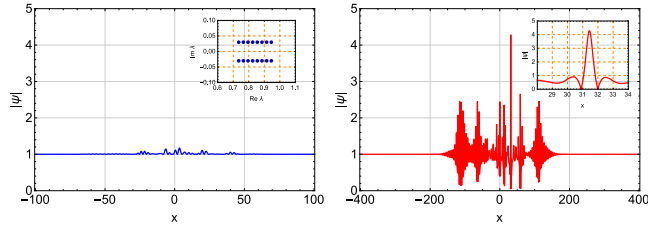


FIG. 4: Rogue wave formation from the condensate locally perturbed by 8 pairs of randomly distributed superregular breathers. The left picture shows the initial conditions at $t = 0$, and the moment of maximum amplitude generation ($t_{max} = 9.042$) is presented on the right. The inset pictures show the breather eigenvalues and a magnification of the generated rogue wave.

The final question of key importance is whether superregular breathers are contained in arbitrary-type SLCP. Indeed, the ability of superregular breathers to produce the broad family of initial conditions was demonstrated many times [18–20], but the inverse task – decomposition of arbitrary initial condensate perturbation into elementary nonlinear modes, including superregular breathers – has not been considered. Here, we study the spectrum of the ZH system (3) for several general types of randomly generated SLCP and demonstrate that superregular pairs of eigenvalues are present in the spectrum.

We use M harmonics with arbitrary phases belonging to the unstable part of the MI growth rate (2) and modulate them with different functions $f(x, \sigma)$ to obtain localized condensate perturbation $\delta\psi$ ($\psi = A + \delta\psi$; σ is the spatial width of the perturbation):

$$\delta\psi(x) = \epsilon \rho f(x, \sigma) \sum_{j=1}^M \sin(k_j x + \varphi_j), \quad (10)$$

$$k_j = k_0 + \Delta k(j - 1 - M/2); \quad \varphi_j \in [0, 2\pi].$$

Here, $\rho = 1$ or i , and ϵ characterizes the perturbation amplitude. We use several harmonics ($M \sim 10$) and vary the modulation functions. Then, we solve the ZH eigenvalue problem (3) using the standard Fourier collocation method [27] with high numerical accuracy. We study the initial perturbation at a large numerical interval of $1024 \cdot \pi$ and use 16384 discretization points (the latter corresponds to the maximum performance of 192 GB RAM). This process enables us to avoid the effect of periodicity (which is manifested by the appearance of finite-gap zones in the eigenvalue spectrum – see the recent preprint [28] – where such a case was described) and unambiguously identify discrete spectrum eigenvalues.

In the simplest case, symmetric superregular breathers (7) at $\theta_1 = \theta_2 = \pi/2$ and an arbitrary (although not necessary small) value of ϵ generate pure imaginary condensate perturbation (note that we assume

that the condensate is the real constant). This can be easily proved by considering a two-breather solution (equation (4) with $N = 2$) with parameters (7) at $t = 0$. Thus, we first study pure imaginary arbitrary-type condensate perturbations, i.e., the case $\rho = i$ in (10). For several random runs with modulation functions $f = \text{sech}(\sigma x)$ and $f = \exp(-x^2/\sigma^2)$, we clearly observe different distributions of symmetric eigenvalues near the branchcut – an example is presented in Fig. 5 (left). In addition, we study pure real perturbations (now one can show using solution (6) that single Kuznetsov-Ma breather generate pure real perturbation at $t = 0$). In this case, we find eigenvalues on the real axes very close to the branch point – see Fig. 5 (right). The latter corresponds to the scenario suggested by V.I. Shrira and V.V. Geogjaev [17] (see the *Introduction*).

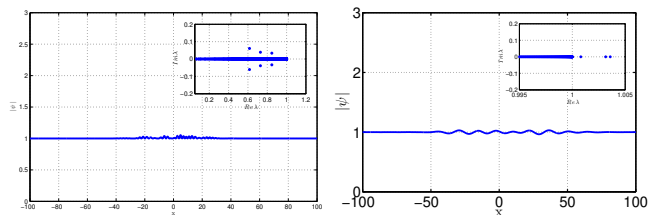


FIG. 5: Eigenvalues of arbitrary-type SLCP. Left: imaginary perturbation generated via (10) with $M = 8$, $k_0 = \sqrt{2}$, $dk = 0.1$, $f(x) = \exp(-x^2/30^2)$ and $\epsilon = 10^{-1}$. Right: real perturbation generated in similar way with $M = 8$, $k_0 = 0.4$, $dk = 0.025$, $f(x) = \exp(-x^2/40^2)$ and $\epsilon = 2 \cdot 10^{-2}$.

Discussion and Conclusion

In this paper, we show that superregular breathers are an important part of the scattering data for arbitrary-type condensate perturbations and play the key role in the formation of rogue waves as a result of MI. We demonstrate that pure imaginary perturbations contain superregular breathers with symmetric eigenvalues, whereas pure real perturbations contain Kuznetsov-Ma breathers with eigenvalues close to the branch point. However, the eigenvalue spectrum does not reveal the impact of the continuous spectrum waves (we also need to study the *reflection coefficient*, see, for instance, [7, 8]). Moreover, the numerical simulation of the evolution of the perturbations presented in Fig. 5 shows complicated wave patterns that are apparently driven by nonlinear interaction between the breathers and continuous spectrum (stable and unstable parts) waves. All these questions demand separate consideration.

Another important task is to study the combinations of imaginary and real perturbations or perturbations based on broadband random noise. For the latter case, B. Kibler et al. found strong signatures of superregu-

lar breathers at the intermediate stage of MI development [29].

Another fundamental problem is the development of MI from spatially periodic perturbations. Recently, important results in this field were obtained by D.S. Agafontsev and V.E. Zakharov, who studied NLSE wavefield statistics on different unstable backgrounds [30, 31]. Furthermore, significant progress was made by J.M. Soto-Crespo, N. Devine and N. Akhmediev, who attributed the formation of rogue waves from the stochastic periodic condensate perturbations to breather collisions [32, 33], and S. Randoux, P. Suret and G. El, who linked these phenomena with the *multi-phase (finite-band)* solutions of the NLSE [34] (see also the paper [35]). We believe that superregular breathers can also appear in such numerical simulations when the size of the numerical tank is significantly larger than the typical width of the superregular perturbations.

Finally, we note that the space-phase shifts describing NLSE breathers collisions found in this paper can be used for further studies, among which the experimental realization of complicated multi-breather dynamics is of special interest.

APPENDIX

Spectral parameter

In our previous works [18–20] we use the so-called Joukowski transform of spectral parameter λ to simplify theoretical analysis of N -breather solutions:

$$\lambda = \frac{A}{2} \left(\xi + \frac{1}{\xi} \right), \quad \xi = r e^{i\alpha} = e^{z+i\alpha}. \quad (11)$$

In such variables the two-sheeted Riemann λ -surface transforms into the one-sheeted ξ -plane. The line of branchcut $[-A, A]$ transforms into a circle of unit radius, while the Riemann sheets become the outer and inner parts of the circle.

In ξ variable the general one-breather solution of the NLSE (1) can be obtained in the following elegant form (compare with Eq. (6)):

$$\psi_1 = A e^{-i\theta_c} N_1 / \Delta_1, \quad (12)$$

$$\begin{aligned} N_1 &= \cosh z \cos 2\alpha \cosh 2u + \cosh 2z \cos \alpha \cos 2v \\ &\quad + i(\cosh z \sin 2\alpha \sinh 2u + \sinh 2z \cos \alpha \sin 2v), \\ \Delta_1 &= \cosh z \cosh 2u + \cos \alpha \cos 2v, \end{aligned}$$

where

$$\begin{aligned} u &= \varkappa(x - x_0) - \gamma t, & v &= \eta x - \omega t - \theta/2, \\ \varkappa &= A \sinh z \cos \alpha, & \gamma &= -A^2 \cosh 2z \sin 2\alpha/2, \\ \eta &= A \cosh z \sin \alpha, & \omega &= A^2 \sinh 2z \cos 2\alpha/2. \end{aligned}$$

Now the Peregrine, Kuznetsov-Ma and Akhmediev breathers correspond to the following parameters: $r = 1, \alpha = 0$; $r > 1, \alpha = 0$; and $r = 1, \alpha \neq 0$. The oscillation period of Kuznetsov-Ma breather is defined by $1/\sinh 2z$ and tends to infinity when this solution transforms to the Peregrine breather (in the limit $r \rightarrow 1$).

The condensate complex phase at infinity should be constant with time for any localized perturbation. Thus, the breather solutions capable to describe the growth of SLCP should have equal condensate phases at $x \rightarrow \pm\infty$, or at least have difference in the phases comparing with the relative amplitude of the initial perturbation. A single breather changes the phase of the condensate before and after itself on 4α , that can be seen considering asymptotics of the expression (12) at $x \rightarrow \pm\infty$ [19].

Among one-breather solutions of the NLSE, only Kuznetsov-Ma and Peregrine breathers have equal condensate phases at infinity. As we discussed in the introduction, these solutions were already considered for description of MI development from SLCP. For a couple of breathers, the total change of phase before and after them is zero when

$$\alpha_1 = -\alpha_2. \quad (13)$$

As was found in the work [18] at certain phase synchronisation (close to $\theta_1 + \theta_2 = \pi$) and when the breather eigenvalues located near the branchcut ($r - 1 \ll 1$), such two-breather solution generate SLCP at an initial moment of time. In the general case SLCP can be formed by \tilde{N} pairs of breathers satisfying the condition $\alpha_{2j-1} = -\alpha_{2j}$; $j = 1, \dots, \tilde{N}$. Such special type of exact solutions are called \tilde{N} -pair superregular breathers.

Eigenvalue parameters of symmetric superregular breather (7) now are written as

$$\alpha_1 = -\alpha_2 = \alpha; \quad r_1 = r_2 = r; \quad r - 1 = \tilde{\varepsilon} \ll 1, \quad (14)$$

In this case, the initial (linear) stage of perturbation growth is described by the following expression obtained in [19]:

$$\delta\psi \approx i\tilde{\varepsilon}A \frac{\cosh(i\alpha - 2\gamma t) \cos(2\eta x - (\theta_1 - \theta_2)/2)}{\cosh((2A\tilde{\varepsilon} \cos \alpha)x)}. \quad (15)$$

Here $\delta\psi$ is the SLCP: $\psi = A + \delta\psi$. The maximum value of the growth rate (defined by 2γ) for the expression (15) is achieved at $\alpha = \pi/4$. In this case superregular breather corresponds to the maximum of the MI growth rate (2), similar to the Akhmediev breather [36]. Indeed, when $\alpha = \pi/4$ ($Re[\lambda] = 1/\sqrt{2}$), maximum of the most significant Fourier spectrum sideband mode is located at $k_{max} = \pm\sqrt{2}$ (with accuracy $\sim \tilde{\varepsilon}$) – see the Fig. 1.

Obviously (13) defines the family of parametric curves given by Eq. (8), that is illustrated here in Fig. 6. The SLCP are formed only by eigenvalues located on the grey (long dashed) and orange (short dashed) lines since the distance between the eigenvalues and the branchcut defines the amplitude of the initial perturbation.

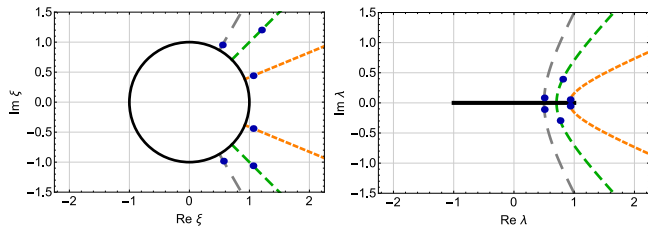


FIG. 6: Comparison of ξ and λ parametrizations of spectral parameter. The branch cut and its Joukowski mapping (11) are drawn by black solid lines. The pairs of breather eigenvalues (marked by blue points) lie on the rays (13) (dashed lines, left picture) and on the parametric curves (8) (dashed lines, right picture).

Breather collisions

Here we discuss synchronization of the four-breather MI development presented by Fig. 3. First we introduce the breather group and phase velocities, that can be obtained from expressions (5):

$$V_{gr} = -\frac{\text{Im}[\lambda_n \cdot \zeta_n]}{\text{Re}[\zeta_n]}, \quad V_{ph} = \text{Re}[\lambda_n \cdot \zeta_n]. \quad (16)$$

We choose the initial moment of time $t_0 = 0$ and the moment of rogue wave formation $t_{max} = 15$ (with maximum amplitude at $x = 0$). The problem is to find initial space shifts and phases for each breather. Let us denote breathers in the left superregular pair (see Fig. 3) by indexes 1 (the breather moving to the left) and 2 (the breather moving to the right) and breathers in the right pair by indexes 3 (the breather moving to the left) and 4 (the breather moving to the right). The breathers 2 and 3 have complex conjugated eigenvalues, so they differ only in the direction of the group velocity: $V_{gr2} = -V_{gr3} = \tilde{V}_{gr}$. Before the moment t_0 , the breather 2 was affected by collisions with the breathers 1 and 4, so the total space shift for the breather 2 can be found as:

$$x_{0,2} = -\tilde{V}_{gr} \cdot t_{max} - \Delta x_{0,12} + \Delta x_{0,42}. \quad (17)$$

Here $\Delta x_{0,12}$ and $\Delta x_{0,42}$ are calculated via space-shift formula (9). To obtain further synchronisation inside the left superregular pair, we choose the same space shift for the breather 1: $x_{0,1} = x_{0,2}$. By analogy we obtain the following space shifts for the breathers 3 and 4:

$$x_{0,3} = x_{0,4} = \tilde{V}_{gr} \cdot t_{max} - \Delta x_{0,13} + \Delta x_{0,43}. \quad (18)$$

Synchronization of phases we start from the breathers 2 and 3. According to the Fig. 2 the phases of both breathers should be equal to π , but we have to account the phase changing with time t_{max} and phase shifts acquired after collisions with breathers 1 and 4. Denoting the phase velocity for the second and third breather as

$V_{ph2} = V_{ph3} = \tilde{V}_{ph}$ we obtain:

$$\theta_2 = \theta_3 = \pi + \tilde{V}_{ph} \cdot t_{max} - \Delta\theta_{12} + \Delta\theta_{42}. \quad (19)$$

Here $\Delta\theta_{12}$ and $\Delta\theta_{42}$ are calculated via phase-shift formula (9). Now the formation of the rogue wave at t_{max} is obtained and we only need to synchronise formation of small condensate superregular perturbations at t_0 . As we discussed in the main text of the paper superregular synchronization appears at $\theta_1 + \theta_2 = \pi$ (see again the Fig. 2). The breather 1 was affected by collisions with the breathers 3 and 4, while the breather 4 collided with breathers 3 and 1. Thus, the required phase shifts can be found as:

$$\begin{aligned} \theta_1 &= \pi - \theta_2 - \Delta\theta_{13} - \Delta\theta_{14}, \\ \theta_4 &= \pi - \theta_3 + \Delta\theta_{43} - \Delta\theta_{14}. \end{aligned} \quad (20)$$

Acknowledgments

The author is thankful to 1) Prof. V.E. Zakharov for providing the idea to study imaginary and real condensate perturbations separately; 2) Prof. E.A. Kuznetsov for the helpful discussions of continuous spectrum waves; 3) Dr. D.S. Agafontsev for the helpful comments with regard to the Fourier spectrum of superregular breathers and discussion of possible applications of the presented results in the interpretation of numerical simulations with periodically perturbed condensate; and 4) Dr. B. Kibler for the helpful discussions of the broadband random noise SLCP. Numerical code and simulations were performed at the Novosibirsk Supercomputer Center (NSU). The most part of the work was performed with support from the Russian Science Foundation (Grant No. 14-22-00174). The study presented in the paragraph "Breather interactions: space-phase shifts" was supported by the RFBR (Grant No. 17-41-543347 r mol a).

* Electronic address: agelash@gmail.com; gelash@srd.nsu.ru

- [1] V. E. Zakharov and L. A. Ostrovsky, *Physica D: Nonlinear Phenomena* **238**, 540 (2009).
- [2] C. Kharif, E. Pelinovsky, and A. Slunyaev, *Rogue waves in the ocean, observation, theories and modeling* (Advances in Geophysical and Environmental Mechanics and Mathematics Series, Springer, Heidelberg, 2009).
- [3] D. R. Solli, C. Ropers, P. Koonath, and B. Jalali, *Nature* **450**, 1054 (2007).
- [4] V. B. Efimov, A. N. Ganshin, G. V. Kolmakov, P. V. E. McClintock, and L. P. Mezhov-Deglin, *Eur. Phys. J. Special Topics* **185**, 181 (2010).
- [5] A. Chabchoub, N. P. Hoffmann, and N. Akhmediev, *Physical Review Letters* **106**, 204502 (2011).
- [6] V. E. Zakharov and A. B. Shabat, *Soviet Physics JETP* **34**, 62 (1972).

- [7] E. A. Kuznetsov, in *Akademiia Nauk SSSR. Doklady*, Vol. 236 (1977) pp. 575–577.
- [8] Y.-C. Ma, *Studies in Applied Mathematics* **60**, 43 (1979).
- [9] T. Kawata and H. Inoue, *Journal of the Physical Society of Japan* **44**, 1968 (1978).
- [10] D. H. Peregrine, *J. Austral. Math. Soc. Ser. B. Appl. Math.* **25**, 16 (1983).
- [11] N. N. Akhmediev, V. M. Eleonskii, and N. E. Kulagin, *Sov. Phys. JETP* **62**, 894 (1985).
- [12] E. Kuznetsov, *JETP letters* **105**, 108 (2017).
- [13] G. Biondini and D. Mantzavinos, *Physical Review Letters* **116**, 043902 (2016).
- [14] G. Biondini, S. Li, and D. Mantzavinos, *Physical Review E* **94**, 060201 (2016).
- [15] N. Akhmediev, A. Ankiewicz, and J. M. Soto-Crespo, *Phys. Rev. E* **80**, 026601 (2009).
- [16] P. Dubard and V. B. Matveev, *Nonlinearity* **26**, R93 (2013).
- [17] V. I. Shrira and V. V. Geogjaev, *J. Eng. Math.* **67**, 11 (2010).
- [18] V. E. Zakharov and A. A. Gelash, *Physical Review Letters* **111**, 054101 (2013).
- [19] A. A. Gelash and V. E. Zakharov, *Nonlinearity* **27**, R1 (2014).
- [20] B. Kibler, A. Chabchoub, A. Gelash, N. Akhmediev, and V. E. Zakharov, *Phys. Rev. X* **5**, 041026 (2015).
- [21] J.-H. Zhang, L. Wang, and C. Liu, in *Proc. R. Soc. A*, Vol. 473 (The Royal Society, 2017) p. 20160681.
- [22] C. Liu, Y. Ren, Z.-Y. Yang, and W.-L. Yang, *Chaos: An Interdisciplinary Journal of Nonlinear Science* **27**, 083120 (2017).
- [23] N. Akhmediev, J. M. Soto-Crespo, and A. Ankiewicz, *Phys. Rev. A* **80**, 043818 (2009).
- [24] N. Akhmediev, J. M. Soto-Crespo, and A. Ankiewicz, *Phys. Lett. A* **373**, 2137 (2009).
- [25] A. Gelash and D. Agafontsev, in *Proceedings of EGU-General Assembly, Vienna, Austria*, Vol. 19 (2017) p. 15446.
- [26] L. Frumin, A. Gelash, and S. Turitsyn, *Physical Review Letters* **118**, 223901 (2017).
- [27] Y. Jianke, *Nonlinear waves in integrable and nonintegrable systems*, Vol. 16 (Society for Industrial and applied Mathematics, Philadelphia, 2010).
- [28] P. Grinevich and P. Santini, arXiv preprint arXiv:1707.05659 (2017).
- [29] B. Kibler, A. Chabchoub, A. Gelash, N. Akhmediev, and V. E. Zakharov, *Nonlinear Guided Wave Optics: A testbed for extreme waves* (IOP Publishing Ltd, Editor: Stefan Wabnitz, to be published).
- [30] D. S. Agafontsev and V. E. Zakharov, *Nonlinearity* **28**, 2791 (2015).
- [31] D. S. Agafontsev and V. E. Zakharov, *Nonlinearity* **29**, 3551 (2016).
- [32] J. M. Soto-Crespo, N. Devine, and N. Akhmediev, *Physical Review Letters* **116**, 103901 (2016).
- [33] N. Akhmediev, J. M. Soto-Crespo, and N. Devine, *Physical Review E* **94**, 022212 (2016).
- [34] S. Randoux, P. Suret, and G. El, *Scientific reports* **6** (2016).
- [35] M. Bertola, G. El, and A. Tovbis, in *Proc. R. Soc. A*, Vol. 472 (The Royal Society, 2016) p. 20160340.
- [36] N. Akhmediev, A. Ankiewicz, J. M. Soto-Crespo, and J. M. Dudley, *Phys. Lett. A* **375**, 775 (2011).